Retrospective Study

Prognostic Effect of Trigeminal Neuralgia Treated With Percutaneous Balloon Compression by Machine Learning-based Modeling of Radiomic Morphological Features

Ji Wu, PhD[1], Keyu Chen, PhD[1],Hao Mei, PhD[2], Yuankun Cai, PhD[1], Lei Shen, BA[1], Jingyi Yang, BA[1], Dongyuan Xu, PhD[1], Songshan Chai, PhD[1], and Nanxiang Xiong, PhD[1]

From: [1]Department of Neurosurgery, Wuhan University Zhongnan Hospital, Wuhan, People's Republic of China; [2]Department of Radiology, Wuhan University Zhongnan Hospital, Wuhan, People's Republic of China

Address Correspondence: Nanxiang Xiong, PhD Department of Neurosurgery, Wuhan University Zhongnan Hospital, Wuhan, 430000, People's Republic of China E-mail: mozhuoxiong@163.com

Disclaimer: J Wu and K Chen contributed equally to this work. There was no external funding in the preparation of this article.

Conflict of interest: Each author certifies that he or she, or a member of his or her immediate family, has no commercial association (i.e., consultancies, stock ownership, equity interest, patent/licensing arrangements, etc.) that might pose a conflict of interest in connection with the submitted article.

Article received: 01-08-2024
Revised article received: 03-14-2024
Accepted for publication: 06-10-2024

Free full article: www.painphysicianjournal.com

Background: Trigeminal neuralgia (TN) is defined as spontaneous pain in the region of the trigeminal nerve that seriously affects a patient's quality of life. Percutaneous balloon compression of the trigeminal ganglion is a simple and reproducible surgical procedure that reduces the incidence of TN, but the postoperative outcome is poor in some patients, with it being ineffective or TN recurring.

Objectives: To establish a machine learning-based clinical imaging nomogram to predict the recurrence of trigeminal neuralgia in patients treated with percutaneous balloon compression.

Study Design: Retrospective study.

Methods: The clinical data of 209 patients with TN treated with percutaneous balloon compression at Zhongnan Hospital of Wuhan University from January 2017 through August 2023 were retrospectively collected and randomized into training and validation cohorts. All imaging histologic morphological features were extracted from the intraoperative x-ray balloon region using 3D slicer software. The relationship among clinical factors, least absolute shrinkage and selection operator, and 4 machine learning predictions of the patient's TN prognosis were analyzed using a one-way analysis of clinical factors. A prediction model was constructed using receiver operating characteristics curve analysis. The performance of the clinical imaging histogram of patients' TN prognoses was evaluated using a receiver operating characteristics curve and decision curve analysis. The model was finally validated using a validation cohort and a receiver operating characteristics curve.

Results: The training group included 149 patients; 16 morphology-related imaging histological features were extracted for analysis. After one-way logistic regression analysis, least absolute shrinkage and selection operator analysis incorporated original_shape_Elongation, original_shape_MajorAxisLength, original_shape_flatness morphology-related imaging histologic features, gender, and affected side to give a total of 6 predictors. The final results were obtained for gender, affected side, and MajorAxisLength. Finally, 4 machine learning receiver operating characteristics curves for random forest tree, support vector machine, generalized linear model, and extreme gradient boosting models were obtained for the clinical and imaging features of gender, affected side, drug, original_shape_MajorAxisLength, and original_shape_flatness. The areas under the receiver operating characteristics curves were 0.990, 0.993, 0.990, and 0.986, respectively. Finally, predictive column maps of affected side, gender, original_shape_flatness, and MajorAxisLength were constructed using the support vector machine method, and the area under the receiver operating characteristics curve of the model was 0.99, which suggests that the model had good predictive ability. Decision curve analysis and calibration curves showed high applicability of column-line diagrams in clinical practice. Our validation cohort consisting of 60 patients had an area under the receiver operating characteristics curve of 0.857.

Limitations: This study was performed in a single center. The nature of this study was retrospective rather than prospective and randomized, and it was not possible to entirely control for nuisance variables.

Conclusion: Screening clinical information by machine learning, combined with a clinical imaging histology nomogram, has good potential for predicting the prognosis of a patient's TN treated

with percutaneous balloon compression, and is suitable for clinical application in patients with TN after percutaneous balloon compression.

Key words: Machine learning, nomogram, percutaneous balloon compression, trigeminal neuralgia, prognosis

Pain Physician 2024: 27:E1105-E1116

Trigeminal neuralgia (TN) is a spontaneous pain sensation that occurs in the trigeminal nerve region; the clinical manifestations are mainly paroxysmal electric shock-like or pinprick-like recurrent pain (1). The initial diagnosis mainly relies on pain symptoms. These symptoms are mainly transient, intense, sudden pain episodes induced by innocuous stimuli such as talking, chewing, or gently touching the overlying skin. The pain site is mainly limited to one or more branches of the trigeminal nerve. Epidemiologically, it has been found that 4–13 individuals per 100,000 are affected each year. Its prevalence is higher in women than in men (2,3).

The main treatment options for TN include drugs and surgery, with the initial treatment of choice being drug therapy. Patients who do not tolerate drugs or whose medical management fails may benefit from surgery (3,4). Currently, the anticonvulsants carbamazepine and oxcarbazepine are the first-line drugs for the treatment of TN, but medication can bring side effects, including drowsiness, dizziness, and skin rash. In addition, patients will often fail to achieve the therapeutic dose of the medication, and should be considered for surgical treatment (1,3). The available surgical treatments include microvascular decompression (MVD) of the trigeminal nerve root, percutaneous neurotomy (radiofrequency thermocoagulation, mechanical balloon compression, and chemical neurotomy), peripheral techniques, radiosurgery, and deep brain stimulation.

Currently, MVD is the preferred surgical treatment for patients with TN who have well-defined vascularized nerves. However, the delicate posterior cranial fossa craniotomy is highly demanding for the surgeon, and postoperative complications such as cranial nerve dysfunction, pain exacerbation, cerebrospinal fluid leakage, and intracranial infections can be serious and lead to patient death (4,5). Conversely, percutaneous balloon compression (PBC) of the trigeminal ganglion is considered an inexpensive and effective alternative, with pain relief rates ranging from 70% to more than 90% (6,7). In recent years, PBC has been characterized by its short operative time, small surgical wounds, and repeatability. Therefore, PBC is increasingly used for patients who do not tolerate other surgical methods. However, some patients still have unsatisfactory postoperative outcomes; there is also a degree of inefficiency and a small recurrence rate (5).

Radiomics is an emerging study methodology that involves high-throughput extraction and analysis of a large number of high-dimensional quantitative image features extracted from medical images from different modalities (8). Its advantage is that it transforms visual image information into deep features for quantitative study (8,9). Moreover, radiomics allows multiple image features to be studied in parallel, and can provide combinations of features, with the analysis of these combined features being more promising than single feature analysis (10).

In relation to the PBC procedure, although deformation of the balloon in the correct position and formation of the correct pear shape, as seen by intraoperative lateral fluoroscopy films, are considered crucial for surgical success, previous studies have found that factors such as TN staging and imaging features, in addition to balloon shape, volume, and compression time, may be associated with the efficacy of PBC in treating TN (11-13). Despite many researchers' attempts to define the shape of the pear, the criteria for becoming a pear shape are still not uniform. Studies have reported the results of correlation analyses between clinical factors and the therapeutic efficacy of TN treatment (6,11,13). Most previous studies focused mainly on the comparative study of clinical data, ignoring the value of imaging histology and histomorphology for predicting disease progression. The predictive value of intraoperative balloon morphology imaging histological features for postoperative recurrence of TN is unclear.

In our study, patient clinical information and imaging histology morphological features extracted from intraoperative balloon x-rays were used to build a predictive model of postoperative TN recurrence. We constructed a model using multifactorial logistic regression analysis, 4 machine learning algorithms, and a nomogram based on columns of clinical risk factors and imaging histology features. The model's reliability was evaluated using calibration curves and decision curve analysis (14,15). Our study is the first to establish a novel scoring system that can be used to predict the

likelihood of postoperative painlessness or recurrence using preoperative and intraoperative characteristics.

Methods

Since this was a retrospective study with anonymized patient data, the Ethics Committee of Zhongnan Hospital of Wuhan University approved a waiver for informed patient consent. Clinical and intraoperative imaging data of patients with TN who underwent PBC at Zhongnan Hospital of Wuhan University from January 2017 through March 2023 were respectively collected. Patients were followed up by telephone to determine if their trigeminal nerve pain had recurred.

Study inclusion criteria were: 1) Age ≥ 18 years; 2) a diagnosis of primary TN; and 3) the availability of complete clinical and imaging data. Exclusion criteria were: 1) those who had undergone MVD; 2) incomplete clinical or imaging data; 3) secondary TN; 4) patients with recurrent TN; and 5) patients who refused follow-up after discharge.

All patients underwent a preoperative 3.0-T skull base magnetic resonance imaging angiography to exclude secondary TN caused by a space-occupying lesion in the cerebellopontine angle cistern area.

The following relevant clinical information was obtained from the patients' medical records: age, gender, facial pain duration, the affected side, trigeminal neuralgia typology, Numeric Rating Scale pain score, carbamazepine's effectiveness, balloon morphology, trigeminal nerve cardiac reflexes, facial numbness, mastication weakness, keratitis, and a score for the compression's severity. Clinical manifestations, such as postoperative surgical response, were confirmed and recorded by a Diagnostic Medical Imaging Physicain.

Finally, 209 patients were included in our study. The patients were randomly split into modeling and validation populations in a 7:3 ratio using R software version 4.2.1 (The R Foundation): 149 for the training cohort and 60 for the validation cohort.

Surgical Procedure

See supplementary materials.

Analysis of the Degree of Vascular Compression Severity Score

According to the 3-dimensional time-of-flight magnetic resonance angiography sequence and T2-weighted imaging sequence, patients were classified as Grade I, Grade II, or Grade III. Grade I is defined as having no vessels surrounding the nerve or having vessels around the nerve without direct touch. Grade II indicates that there is some compression of the nerve by vessels, but not enough to be a distortion of the nerve. Grade III indicates that blood vessels are compressing the trigeminal nerve, causing it to lose its normal shape and become distorted and deformed. Grading was carried out by 2 authors after a period of training by the senior author, and after high reliability and intra-reliability between paired datasets had been achieved. The examiners were blind to clinical outcomes. Grade I was defined as mild vascular compression and Grades II and III as severe vascular compression, according to the criteria of previous studies (16).

Trigeminal Neuralgia Staging

Diagnosis was based on the International Classification of Headache Disorders, 3rd edition (16). TN was dichotomized into classic TN and all other types of TN according to the criteria developed by the International Association for the Study of Pain.

Outcome Assessment

The degree of pain relief was finely assessed by standardized telephone follow-up of patients 180 days post discharge, using the Barrow Neurological Institute (BNI) criteria (Grades I-V) (16,17). We defined Grades I-III as pain relief and Grades IV and V as ineffective pain relief.

Intraoperative Balloon x-ray Image acquisition and Data Collection

All patients underwent intraoperative cranial x-ray fluoroscopy scanning using a Philips UNIQ FD20/20 C-arm (Koninklijke Philips N.V.). The patients were placed supine on the operating table. Their heads were placed on the operating table with their 2 external ear holes equidistant from the examination table. After the balloon was determined to be pear-shaped, lateral film fluoroscopy was performed and the images were collected.

Image Segmentation and Feature Extraction

Interobserver agreement for feature extraction was evaluated using intraoperative cranial x-ray images from randomly selected patients. Hematoma contouring was performed manually and independently by 2 experienced radiologists (film readers one and 2), without knowledge of the clinical data. The reproducibility of interobserver outlining of the region of interest (ROI) was evaluated using an intragroup correlation coefficient. Figure 1 shows an example of the ROI drawings. All im-

age histological features were extracted using 3D Slicer software 4.13 (Slicer Community). Volume and shape features (2D and 3D) were extracted from each ROI.

Imaging Histological Feature Screening and Model Construction

One-way analyses were performed using R software version 4.2.1 and clinical traits and imaging histologic features that were statistically different in a single factor were included in a least absolute shrinkage and selection operator (LASSO) regression analysis to remove overfitting. Four machine learning algorithms—an extreme gradient boosting (XGB) model, random forest (RF) tree model, generalized linear model (GLM), and support vector machine (SVM) model—were then constructed, and the residuals and inverse cumulative distributions of the diagnoses of each algorithm were plotted, as well as the area under the curve (AUC) of the receiver operating characteristic curve (ROC).

The best feature models for machine learning were selected based on the inverse cumulative scores of the residuals and the AUC values of the ROC curve. A column line graph of the best predictive model was plotted using the root mean square package. Calibration curves and decision curve analysis were used to assess the reliability of the models, and finally, the diagnostic ability of the models was verified using the ROC curves of the internal validation cohort (the AUC of the ROC curves was greater than 0.5, and the diagnostic test had some diagnostic value). In addition, as the area under the ROC curve became closer to one, the diagnostic test became more realistic.

Statistical Analysis

R software version 4.2.1 was used for statistical analysis and data processing. Count data are expressed as percentages and measurement data are expressed as mean ± SD. Comparisons between groups were made using a t test or χ^2 test. *P* values < 0.05 were considered statistically significant.

Results

Clinical Characteristics

A total of 149 patients with TN were included

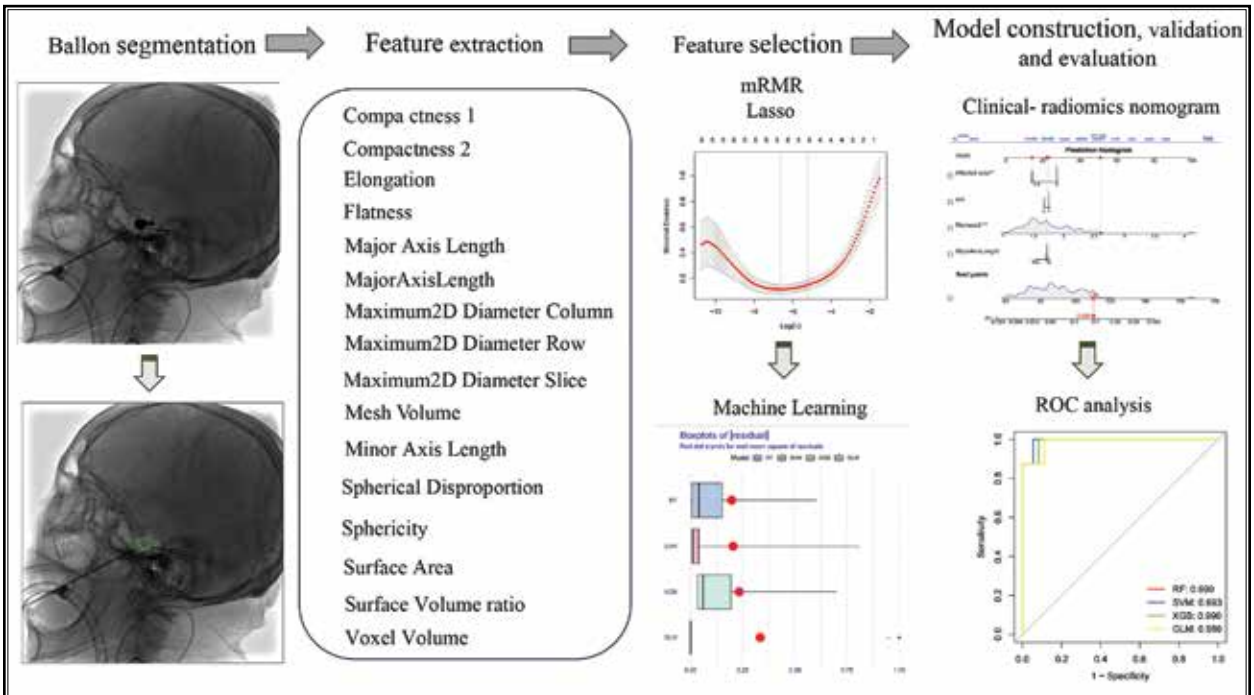

Fig. 1. *Overall workflow of the study.*
An ROI was manually drawn on the lateral plain film. Radiomic features were extracted from the radiographs to quantify their shape characteristics. LASSO and mRMR machine learning algorithms were used to select radiomic features. A nomogram was created for individualized assessment, followed by ROC curve and decision curve analysis.
ROI, region of interest; mRMR, maximum relevance-minimum redundancy; LASSO, least absolute shrinkage and selection operator; ROC, receiver operating characteristics.

in the training cohort (57 men and 92 women; mean age 67.26 ± 10.09 years; age range 48-95 years). The Barrow Neurological Institute scores were I–III in 112 (75.2%) patients and IV and V in 37 (24.8%) patients during the 180-day follow-up. A total of 60 patients were included in the validation cohort (21 men and 57 women; mean age 67.60 ± 9.57 years; age range 44-87 years). Table 1 summarizes the clinical characteristics of the patients.

There were 27 patients in the training cohort ineffective group and 122 in the effective group. There was no statistically significant difference between the 2 groups in terms of age, duration of symptoms, affected side, Numeric Rating Scale score, trigeminal heart reflex, drug response, facial numbness, or keratitis (Table 1). In the effective group, the 81.1% (99 patients) rate for the classic TN type was significantly higher than the 59.3% in the ineffective group (16 patients). Similar results were obtained for the training cohort. In the effective group, 23 (18.9%) patients with the classic TN type were found, which was significantly higher than the rate in the ineffective group (9 cases, 33.3%).

Univariate Analysis of Trigeminal Neuralgia Outcomes

The relationship between clinical traits and TN prognosis was analyzed using one-way logistic regression applied to the training and validation cohorts. As shown in Tables 2 and 3, we observed significant correlations ($P < 0.05$) between gender, TN type, and TN

Table 1. *The clinical characteristics of the training cohort and the validation cohort.*

Characteristics	Training Cohort (n = 149)		*P*	Validation Cohort (n = 60)		*P* Value
	Unfavorable Outcome (n = 27)	Favorable Outcome (n = 122)		Unfavorable Outcome (n = 11)	Favorable Outcome (n = 49)	
Gender			0.006			0.029
Women	16	76		8	18	
Men	11	46		3	31	
Age (years)	67.26 ± 10.09	70.09 ± 9.17	0.157	66 ± 11.43	67.96 ± 9.27	0.547
Affected side			0.008			0.184
Left	5	28		2	23	0.036
Right	22	94		9	26	
Symptom duration (mos)	95. 3 ± 119.621	89.64 + 136.328	0.843	105.09 ± 118.07	142.55 ± 635.61	0.847
Trigeminal affected area			0.208			0.85
V1		6		1	7	
V2	7	16		2	3	
V3	4	16		2	9	
V1+V2	8	24		3	6	
V2+V3	3	39		2	11	
V1+V3		1			9	
V1+V2+V3	5	20		1	4	
Compress severity score			0.559			0.348
No vessel near nerve or Grade I	21	67		9	23	
Grade II or Grade III	6	55		2	16	
Trigeminal Neuralgia type			0.024			0.036
Classic	16	99		9	23	
Secondary and Idiopathic	11	23		2	26	
Therapeutic effect of drug			0.046			0.041
No response to medical treatment	19	60		8	26	
Multiple side effects on drugs	8	62		3	23	

Table 1 cont. *The clinical characteristics of the training cohort and the validation cohort.*

Characteristics	Training Cohort (n = 149)		*P*	Validation Cohort (n = 60)		*P* Value
	Unfavorable Outcome (n = 27)	Favorable Outcome (n = 122)		Unfavorable Outcome (n = 11)	Favorable Outcome (n = 49)	
Intraoperative trigeminal cardiac reflex			0.44			0.882
No	7	41		8	19	
Yes	20	81		3	30	
Postoperative complications						
Facial numbness			0.6			0.833
No	14	70		6	25	
Yes	13	52		5	24	
Keratitis			0.45			0.744
No	23	110		9	42	
Yes	4	12		2	7	

Table 2. *Training cohort. Univariate and multivariate logistic analyses of prognostic risk factors for trigeminal neuralgia.*

Variable	Univariate Logistic Analysis				Multivariate Logistic Analysis			
	Odds Ratio	(95% CI)		*P* value	Odds Ratio	(95% CI)		*P* Value
Gender	0.88	0.38	2.11	0.04	0.94	0.40	2.31	0.048
Age	0.97	0.93	1.01	0.2				
Affected side	1.136	0.997	1.004	0.81				
Trigeminal division	1.001	0.988	1.01	0.881				
Compression severity score	0.78	0.44	1.37	0.4				
Trigeminal neuralgia type	3.31	1.33	8.13	0.009	3.29	1.32	8.12	0.010
Intraoperative trigeminal cardiac reflex	1.45	0.59	3.94	0.4				
Facial numbness	1.25	0.54	2.90	0.6				
Therapeutic effect of drugs	0.44	0.17	1.04	0.07				
Keratitis	1.59	0.42	5.06	0.5				

Table 3. *Test cohort. Univariate and multivariate logistic analyses of prognostic risk factors for trigeminal neuralgia.*

Variable	Univariate Logistic Analysis				Multivariate Logistic Analysis			
	Odds Ratio	(95% CI)		*P* value	Odds Ratio	(95% CI)		*P* value
Gender	0.22	0.04	0.86	0.0391	0.14	0.03	0.63	0.016
Age	0.98	0.91	1.05	0.5				
Affected side	0.2	0.03	0.86	0.051				
Trigeminal division	1.251	1.088	1.21	0.881				
Compression severity score	0.53	0.20	1.28	0.2				
Trigeminal neuralgia type	0.20	0.03	0.86	0.05	0.13	0.02	0.63	0.022
Intraoperative trigeminal cardiac reflex	1.11	0.29	4.70	0.9				
Facial numbness	0.87	0.22	3.25	0.8				
Therapeutic effect of drugs	0.24	0.05	0.93	0.051				
Keratitis	0.33	0.18	6.71	0.7				

outcome in both the training and validation cohorts. Women accounted for the majority of patients who relapsed; typical TN was a significant predictor of immediate TN remission. The univariate analysis shows an OR of 3.31 with a 95% CI of 1.33-8.13 and a *P*-value of 0.009, while the multivariate analysis shows an OR of 3.29 with a 95% CI of 1.32-8.12 and a *P*-value of 0.010, both suggesting a significant association. The results of the validation cohort were broadly consistent with those of the training cohort (Table 3).

Feature Selection for Radiomics and Clinical Traits.

First, 3 radiomics features were extracted differentially from the depicted ROIs. The interobserver intragroup correlation coefficients ranged from 0.751-0.997, so these features had good reproducibility. Next, the 3 best radiomics features were selected from the ROI by maximum relevance-minimum redundancy and LASSO, with these being original_shape_Elongation, original_shape_MajorAxisLength, and original_shape_flatness (Fig. 2).

Machine Learning to Build Diagnostic Models and Validation

We performed a LASSO regression analysis of clinical traits and imaging histological morphological features that differed by a single factor (Figs. 3A, 3B), and finally filtered it to obtain gender, affected side, therapeutic effect of drugs, original_shape_MajorAxisLength, original_shape_flatness, and 5 other traits. Then a trait diagnostic model was built using the RF tree, SVM, XGB, and GLM algorithms. Residuals box

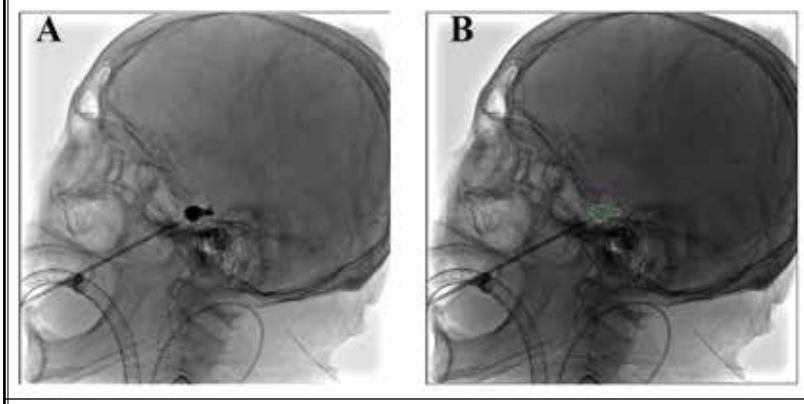

Fig. 2. *Image morphological feature extraction.*
A,B A region of interest was manually drawn on the lateral plain film. Radiomic features were extracted from the radiographs to quantify their shape characteristics.

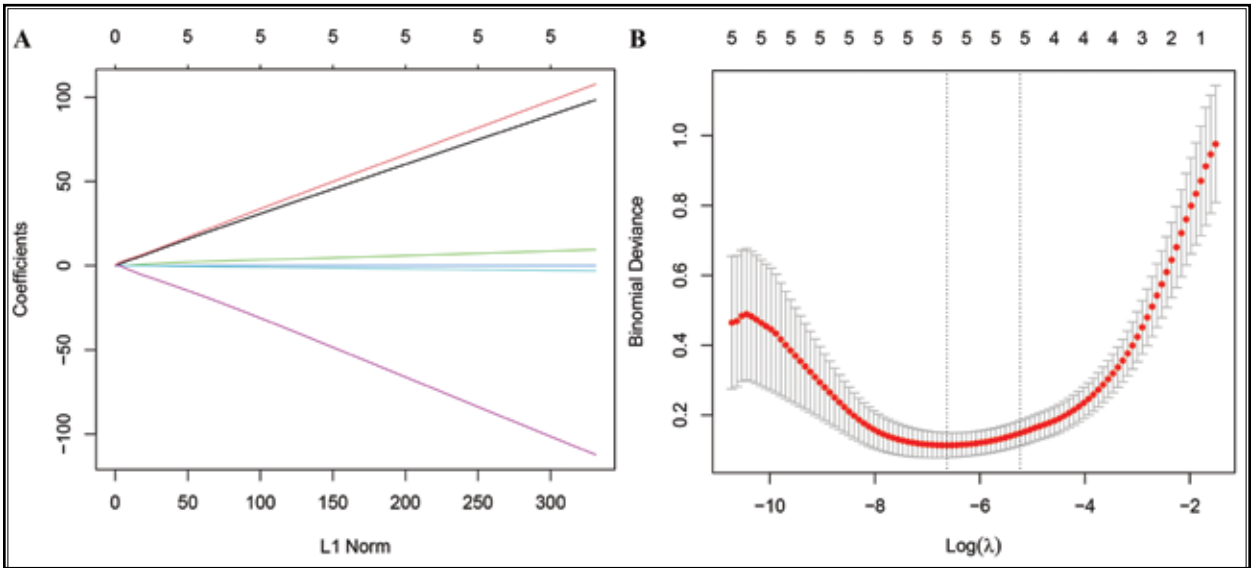

Fig. 3. *Texture feature selection using least absolute shrinkage and selection operator (LASSO) logistic regression. (a) The optimal tuning parameter (λ) was selected using 10-fold cross-validation in the LASSO regression model; (b) LASSO regression coefficient distribution.*

plots of the 4 algorithms arranged in the order of RF < SVM < XGB < GLM are shown in Fig. 4A, with red dots denoting the root-mean-square of the residuals.

The inverse residuals cumulative distributions of the 4 algorithms were plotted (Fig. 4B), and the model constructed by SVM was found to be smaller than that of the majority of the samples with smaller residuals. The 4 models were validated with ROC curves. The AUC values of the 4 models were: RF = 0.990; SVM = 0.993; XGB = 0.990; and GLM = 0.986 (Fig. 4C). The ROC curves of each feature in the model are shown, and their AUC values are: original_shape_MajorAxisLength = 0.674, original_shape_flatness = 0.709, gender = 0.734, and affected side = 0.865 (Fig. 4D). The diagnostic model constructed from the 4 features screened by SVM was validated, and the ROC curves in the training and validation cohorts had AUC values greater than 0.85 (Figs. 4E,4F).

Establishment of the Clinical-radiomics Model

The preoperative clinical and imaging features of gender, affected side, original_shape_MajorAxisLength, and original_shape_flatness from the SVM-screened model were incorporated to predict the risk of TN recurrence. A column-line graph predicting the probability of effective regression after PBC in patients with TN was established (Fig. 5); calibration curves also showed satisfactory agreement (Fig. 6A). The decision curve for the probability of effective outcome in the column-line diagram showed good performance in terms of clinical application. The decision curves showed that if the threshold probabilities were 25% and 95%, respectively, it meant that the column-line diagrams in the study predicting the risk of effective outcomes added more benefit than the all-or-none scenario (Fig. 6B).

Discussion

TN is a type of neuropathic pain characterized by sudden electric shocks or tingling in specific areas of the face (1,4). Although TN is not life-threatening to the patient and the pain subsides completely within a day, the normal life and work of the patient are severely affected by the chronic onset of the pain, which leads to dysfunction in severe cases (2). MVD is widely considered the preferred surgical choice for primary TN if drug therapy fails.

However, MVD is a treatment with surgical risks and mortality. PBC is widely used in treating TN because it is minimally invasive, inexpensive, and relatively easy to perform. PBC relieves trigeminal nerve pain by damaging myelinated axons engaged in triggering pain-related sensory nerves, thereby causing focal axonal injury and demyelination, and blocking abnormal discharge pathways (18). The advantage of selective damage to sensory fibers makes PBC more suitable for primary TN than other ablative procedures. In addition, the procedure can be performed under local anesthesia and does not require an awake sensory test (19,20). Previous studies showed immediate postoperative pain relief rates of PBC for TN of 82%-97.1%, and that the duration of pain relief is about 18-20 months. However, axonal myelin sheaths regenerate, which may be a pathological factor behind pain recurrence after PBC for TN (5,11,21).

The most common complication following PBC is facial numbness. The recovery of facial sensation, indicating the resolution of numbness, is an important sign that the trigeminal ganglion has been adequately compressed and that the procedure has been successful. Other complications include bite muscle weakness, herpes labialis, and keratitis.

Some studies found a correlation between clinically relevant factors and the PBC's effectiveness for treating TN, but no study had examined the role of radiomics in predicting PBC's effectiveness for treating TN (21-23). Some studies found that factors such as preoperative symptom duration, drug response, TN type, and imaging characteristics, as well as intraoperative balloon compression time, intraoperative trigeminal reflexes, balloon shape, and balloon volume, were associated with the prognosis of patients with TN post-PBC (22-24). However, none of the previous studies systematically included radiological features in the prognosis of patients undergoing PBC, particularly the radiological histological features related to morphology.

Previous studies showed that other types of TN are correlated with an increased risk of pain recurrence or lack of satisfactory pain relief (11,25). In our study, we found similar lower pain relief rates in patients with other types of TN. Previous studies showed that vascular and trigeminal nerve compression is detectable on magnetic resonance imaging in up to 78% of patients with TN, and that all patients had evidence of intraoperative neurovascular compression (26). Earlier studies showed that neurovascular compression seen on magnetic resonance imaging is a predictor of prognosis post-PBC (27), although a retrospective analysis found that severe venous compression was associated with a

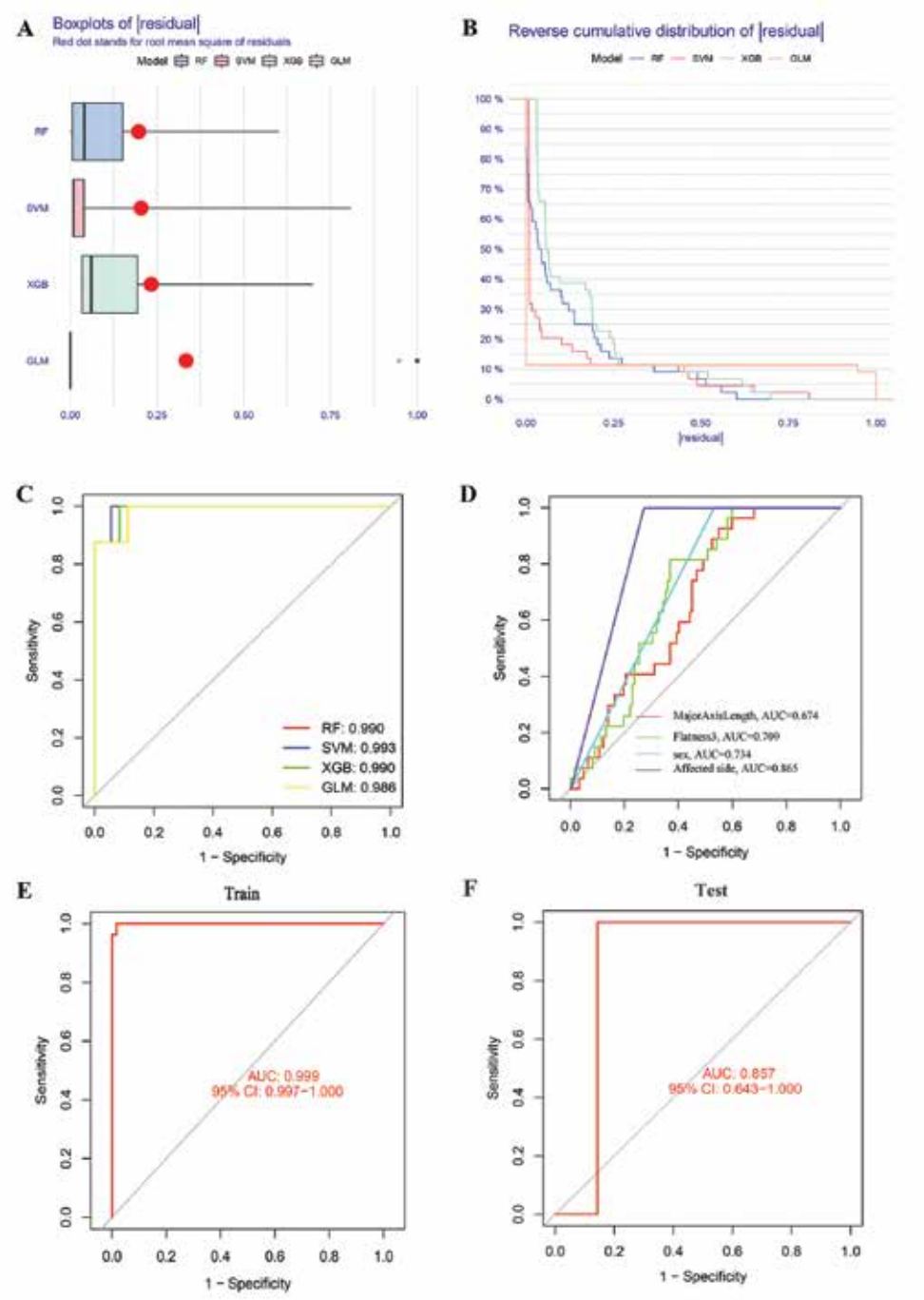

Fig. 4. *Machine learning modelling.*
(A) Inverse cumulative distributions of SVM, RF tree, GLM, and XGB residuals. (B) Inverse cumulative distributions of SVM, RF tree, GLM, and XGB residuals. Y-axis values represent percentiles of outliers. (C) ROC analysis of SVM, RF tree, GLM, and XGB. (D) ROC analysis of affected side, gender, flatness should this be original_shape_flatness ? }, and MajorAxisLength. (E) ROC analysis of the diagnostic model applied to the training cohort. (F) ROC analysis of the diagnostic model applied to the validation cohort.
GLM, generalized linear model; RF, random forest; XGB, extreme gradient boosting; SVM, support vector machine; ROC, receiver operating characteristic curve

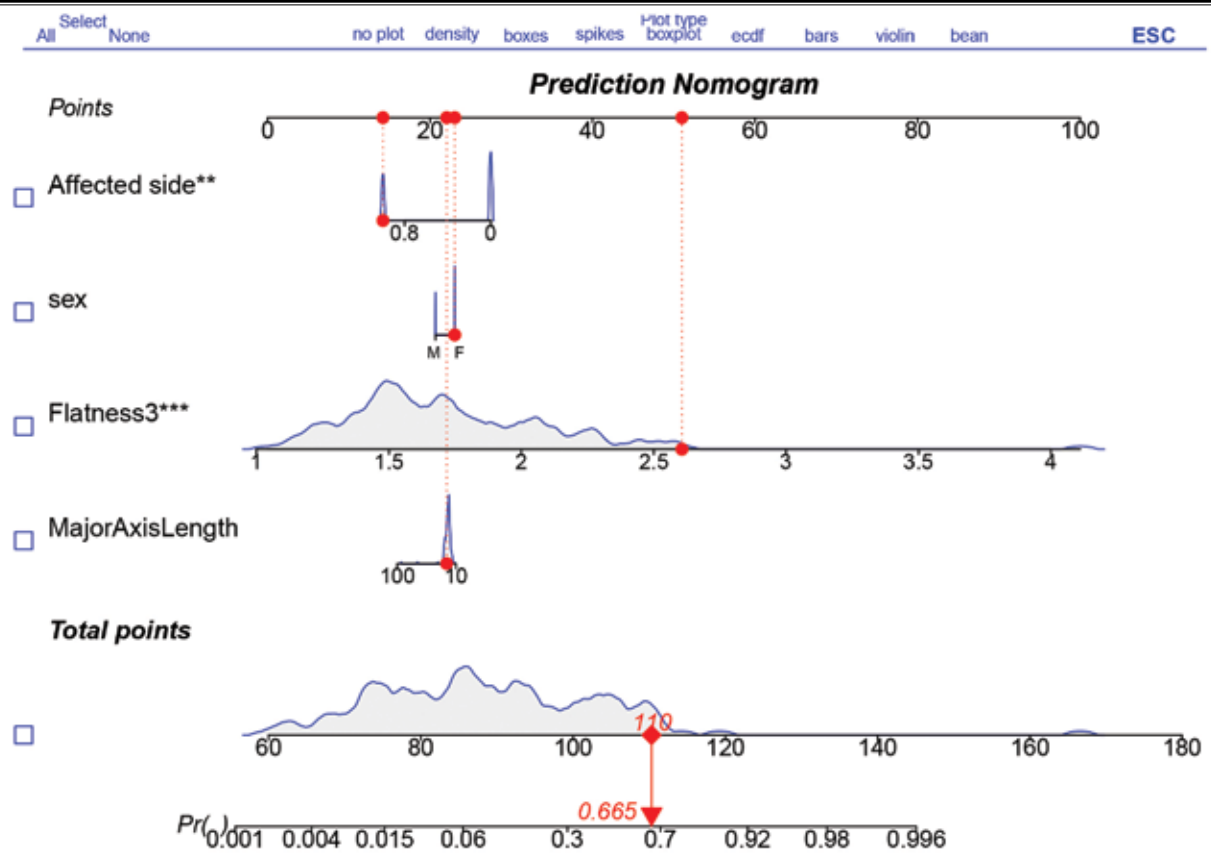

Fig. 5. *Nomogram constructed to predict the probability of recurrent trigeminal neuralgia progress. The values of each variable (affected side, gender, flatness should this be original_shape_flatness ? }, and MajorAxisLength) are summed to obtain a total score.*

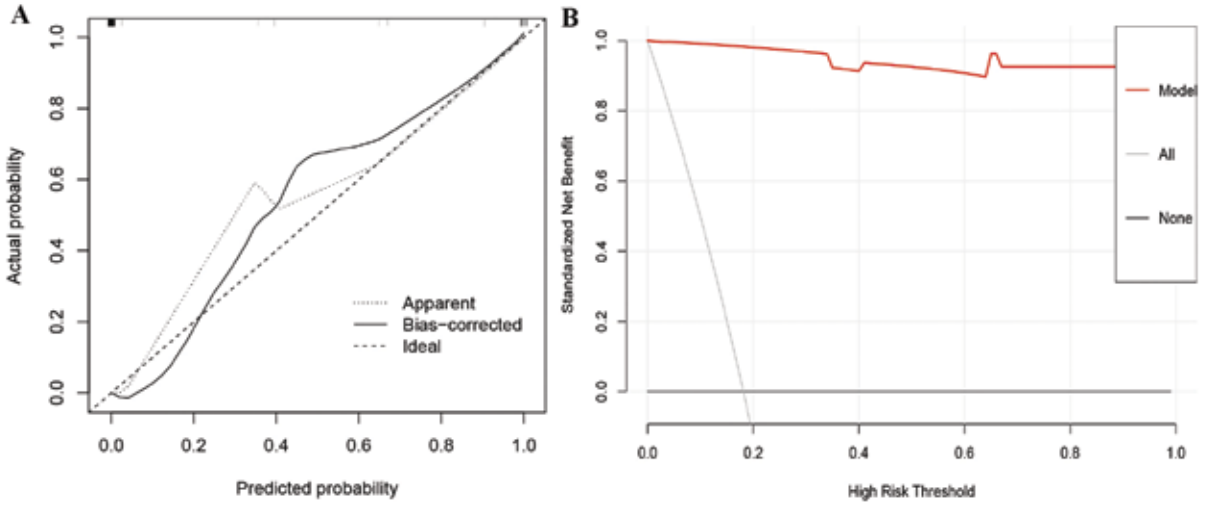

Fig. 6. *Nomogram prediction performance verification. A. The calibration curves of the nomogram. B. The decision curve analysis shows the clinical decision benefit of this model.*

poor prognosis after MVD (28). In our study, we found similar results, with Grade II or Grade III compression severity scores having a higher risk of ineffective pain relief than avascular or Grade I compression severity scores at the 6-month postsurgery follow-up. .

Radiomics, a novel noninvasive image analysis technique, can transform medical images into mined data from which high-dimensional quantitative features can be extracted. The main advantage of radiomics over traditional structural imaging is that these high-dimensional quantitative features can be combined with artificial intelligence applications to construct predictive models that greatly improve clinicians' evidence-based disease diagnosis and prediction efficacy (8,28,29). To date, no study has applied radiomics to predict the efficacy of PBC for TN. In terms of morphology, balloon shape is usually considered an important predictor for determining the efficacy and prognosis of PBC in treating TN (13,21). A pear-shaped balloon seen during PBC is significantly associated with early pain relief rates and significantly longer postsurgery pain-free survival compared with other shapes. However, the optimal pear shape of the balloon depends mainly on the subjective judgment of the surgeon; there is no uniform standard.

In our study, the most relevant radiomic features were extracted from intraoperative x-ray images, and the two most important imaging features were selected. Notably, original_shape_flatness is an important imaging feature and is a radiomics feature that can predict the prognosis of TN post PBC treatment. This characteristic parameter reflects the nonuniformity and original_shape_flatness of the Meckel cave structure, which is related to the pathogenesis of TN (30).

On the basis of these clinically relevant risk factors and radiomics features, an accurate model for predicting review was constructed by LASSO, a machine-learning computation method, to establish a clinical-radiomics model to predict the efficacy and prognosis of the PBC procedure in patients with TN. The AUC of the model was 0.999, which represents very good performance. Validation on the validation cohort, for which the AUC was 0.857, indicated that the discrimination of the model was reasonable. The calibration curve was in good agreement with the decision curve analysis, and the model therefore has potential clinical application.

Limitations

Our study has several limitations. First, this is a single-center retrospective study with a small sample size; larger population samples are needed for large-scale studies. Our next research effort will be to study the trigeminal nerve map through imaging omics, to look for new areas of compression.

Conclusions

In our study, a clinical radiomics model involving machine learning screening of radiomics features and clinical correlates was developed, and a nomogram was constructed to predict the efficacy of PBC in patients with TN. ROC analysis and decision curves showed that the nomogram had good performance in clinical applications and has potential value in precision medicine, where it can help clinicians make clinical therapeutic decisions in patients with a poor prognosis and better achieve postsurgical individualized precision therapy.

Acknowledgments

We thank Liwen Bianji (Edanz) (www.liwenbianji.cn) for editing the language of a draft of this manuscript.

Ethical Approval

This retrospective study was reviewed and approved by the Research Ethics Committee of Zhongnan Hospital, Wuhan University.

Authors Contributions

JW, KC, SC, and NX contributed to the study concept and design. All authors collected the data. JW, KC, and SC contributed to the figure preparation and manuscript review. All authors participated in drafting and approving the final manuscript.

References

1. Cruccu G, Di Stefano G, Truini A. Trigeminal neuralgia. *N Engl J Med* 2020; 383:754-762.
2. Bendtsen L, Zakrzewska JM, Heinskou TB, et al. Advances in diagnosis, classification, pathophysiology, and management of trigeminal neuralgia. *Lancet Neurol* 2020; 19:784-796.
3. Maarbjerg S, Di Stefano G, Bendtsen L, et al. Trigeminal neuralgia - diagnosis and treatment. *Cephalalgia* 2017; 37:648-657.
4. Andersen ASS, Heinskou TB, Rochat P, et al. Microvascular decompression in trigeminal neuralgia - a prospective study of 115 patients. *J Headache Pain* 2022; 23:145.
5. Mizobuchi Y, Nagahiro S, Kondo A, et

al. Microvascular decompression for trigeminal neuralgia: A prospective, multicenter study. *Neurosurgery* 2021; 89:557-564.

6. Xia Y, Yu G, Min F, et al. The focus and new progress of percutaneous balloon compression for the treatment of trigeminal neuralgia. *J Pain Res* 2022; 15:3059-3068.
7. De Cordoba JL, Garcia Bach M, Isach N, et al. Percutaneous balloon compression for trigeminal neuralgia: Imaging and technical aspects. *Reg Anesth Pain Med* 2015; 40:616-622.
8. Zhang YP, Zhang XY, Cheng YT, et al. Artificial intelligence-driven radiomics study in cancer: The role of feature engineering and modeling. *Mil Med Res* 2023; 10: 22.
9. McCague C, Ramlee S, Reinius M, et al. Introduction to radiomics for a clinical audience. *Clin Radiol* 2023; 78:83-98.
10. Huang EP, O'Connor JPB, McShane LM, et al. Criteria for the translation of radiomics into clinically useful tests. *Nat Rev Clin Oncol* 2023; 20:69-82.
11. Kourilsky A, Palpacuer C, Rogers A, et al. Multivariate models to predict pain recurrence and sensitive complications after percutaneous balloon compression in trigeminal neuralgia. *J Neurosurg* 2022; 137:1396-1405.
12. Lv W, Hu W, Chi L, et al. Factors that may affect recurrence of trigeminal neuralgia after percutaneous balloon compression. *J Clin Neurosci* 2022; 99:248-252.
13. Unal TC, Unal OF, Barlas O, et al. Factors determining the outcome in trigeminal neuralgia treated with percutaneous balloon compression. *World Neurosurg* 2017; 107:69-74.
14. Iasonos A, Schrag D, Raj GV, et al. How to build and interpret a nomogram for cancer prognosis. *J Clin Oncol* 2008; 26:1364-1370.
15. Fang C, An X, Li K, et al. A nomogram based on CT radiomics and clinical risk factors for prediction of prognosis of hypertensive intracerebral hemorrhage. *Comput Intell Neurosci* 2022; 2022:9751988.
16. Jannetta PJ. Arterial compression of the trigeminal nerve at the pons in patients with trigeminal neuralgia. *J Neurosurg* 1967; 26:Suppl:159-162.
17. Headache Classification Committee of the International Headache Society (IHS) The International Classification of Headache Disorders, 3rd edition. *Cephalalgia* 2018; 38:1-211.
18. Sterman-Neto H, Fukuda CY, Duarte KP, et al. Balloon compression vs radiofrequency for primary trigeminal neuralgia: A randomized, controlled trial. *Pain* 2021; 162:919-929.
19. Ying X, Wang H, Deng S, et al. Long-term outcome of percutaneous balloon compression for trigeminal neuralgia patients elder than 80 years: A STROBE-compliant article. *Medicine (Baltimore)* 2017; 96:e8199.
20. Chen JF, Tu PH, Lee ST. Long-term follow-up of patients treated with percutaneous balloon compression for trigeminal neuralgia in Taiwan. *World Neurosurg* 2011; 76:586-591.
21. Wang Q, Chen C, Guo G, et al. A prospective study to examine the association of the foramen ovale size with intraluminal pressure of pear-shaped balloon in percutaneous balloon compression for trigeminal neuralgia. *Pain Ther* 2021; 10:1439-1450.
22. Ding Y, Wang Y, Wang Y, et al. A retrospective study to examine the association of different pear-shaped balloons with efficacy and postoperative complications in percutaneous balloon compression for trigeminal neuralgia. *Neurosurg Rev* 2023; 46:60.
23. Asplund P, Linderoth B, Bergenheim AT. The predictive power of balloon shape and change of sensory functions on outcome of percutaneous balloon compression for trigeminal neuralgia. *J Neurosurg* 2010; 113:498-507.
24. Cheng R, Wang T, Cai Y, et al. The consistency between the preoperative 3D-reconstructed Meckel's Cave and the intraoperative balloon results in percutaneous balloon compression. *J Pain Res* 2023; 16:2929-2937.
25. Chen JF, Tu PH, Lee ST. Repeated percutaneous balloon compression for recurrent trigeminal neuralgia: A long-term study. *World Neurosurg* 2012; 77:352-356.
26. Jani RH, Hughes MA, Gold MS, et al. Trigeminal nerve compression without trigeminal neuralgia: Intraoperative vs imaging evidence. *Neurosurgery* 2019; 84:60-65.
27. Liu M, Tang S, Li T, et al. Prognostic nomogram for percutaneous balloon compression in the treatment of trigeminal neuralgia. *Neurosurg Rev* 2022; 45:561-569.
28. Gillies RJ, Kinahan PE, Hricak H. Radiomics: Images are more than pictures, they are data. *Radiology* 2016; 278:563-577.
29. Castiglioni I, Gallivanone F, Soda P, et al. AI-based applications in hybrid imaging: How to build smart and truly multi-parametric decision models for radiomics. *Eur J Nucl Med Mol Imaging* 2019; 46:2673-2699.
30. Lin J, Zhang Y, Li W, et al. Flatness of the Meckel cave may cause primary trigeminal neuralgia: A radiomics-based study. *J Headache Pain* 2021; 22:104.